Highlights

- A novel method of studying *Gammarus pulex* moult cycle using X-ray micro-CT was developed.
- This radiological method compares favourably with other existing published methods of studying moult cycle staging.
- Greater integument calcification is seen in moult stage C compared to stages D and late-D.

Graphical Abstract

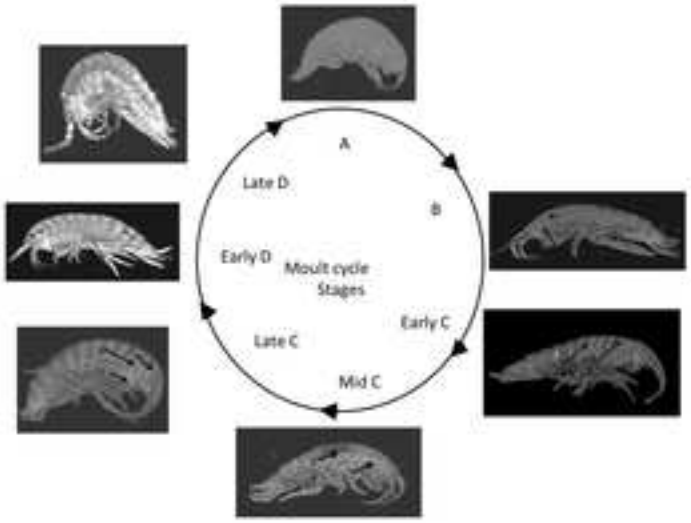

Use of X-ray micro-computed tomography to study the moult cycle of the freshwater amphipod *Gammarus pulex*.

Duncan Bell[1], Nic Bury[1*], Lewis Woolnough[2], Nick Corps[3], David Mortimore[4], Svetlana Gretton[1]

[1]Faculty of Science, Technology and Engineering, University of Suffolk, James Hehir Building, University Avenue, Ipswich, TreviSuffolk IP3 0FS, UK.

[2]Queckett Microscopical Club, c/o The Natural History Museum, Cromwell Rd, London, SW7 5BD, UK.

[3]Bruker UK, Banner Lane, Coventry CV4 9GH, UK.

[4]Newbourne Solutions, Newbourne, Woodbridge IP12 4NR, UK.

- **Corresponding author: n.bury@uos.ac.uk**

Abstract

Stages of the moult cycle of the amphipod *Gammarus pulex* have been previously characterised based on the examination of either apolysis of the 3rd dactyl, or the whole body and eye appearance. In the current study the aim was to compare these two established moult staging techniques with a novel X-ray micro-computed tomography (micro-CT) scan method. The micro-CT provides information on the degree of calcification of the external integument and of the internal structures, such as the gastric mill. The degree of calcification is predicted to change during the moult cycle. Successful micro-CT scans were obtained from 80 *G. pulex* specimens and the radiological appearance of the 28 specimens immediately immersed in 4 % PFA were not different to the 52 specimens stored in 4 % PFA for at least 28 days prior to scanning. These specimens could be classified into moult stages A, B, C, early D or late D based on the degree of calcification. Good agreement was obtained between all three methods of moult stage classification if fresh specimens were used, but if specimens had been preserved in 4% Paraformaldehyde (PFA) for more than 24 hours the loss of colour from the whole body and eye meant these methods were not suitable. This is the first time that a micro-CT method has been used to study *G. pulex* and shows that this method of moult staging is accurate and reliable.

Key Words

Amphipod; moult cycle; micro-computerised tomography, CT-scan

1. Introduction

The moult cycle, which is under endocrine control, is essential for crustacean growth affecting both the outer integument and internal organs. Trevisan et al., (2014) showed that moulting individuals stop feeding, and thus the process interferes with the digestive tract. It is thus critical that experimental studies of crustacean physiology or their response to abiotic or biotic stressors consider the stage an organism is at in their moult cycle at the point of study.

Several studies have divided the moult cycle of crustaceans into 5 basic stages: A, B, C, D1 and D2 (Cornet et al., 2012**;** Trevisan et al., 2014). The classification by Trevisan et al., (2014) is based on external morphological features such as body colour, presence or absence of gut contents and red-orange lipid storage droplets along the posterior borders of the tergites and coxal plates, as well as eye colour changes. They describe that just after the moult (stage A), the exoskeleton was soft and the specimen a greyish yellow colour with few lateral red-orange dots of stored lipids and predominantly white eyes sometimes speckled with black dots. Specimens in late post-ecdysis (stage B) were described as greyish to greenish colour with blackening of the eyes speckled with white spots, but no remaining red-orange lateral lipid dots. Very late post-ecdysial to anecdysial specimens (stage C) are described as having a fully rigid cuticle that appeared greenish coloured with predominantly black eyes although occasionally still flecked with white spots. Early pre-ecdysial specimens (stage D1) had completely black eyes, were olive green in colour with many obvious rows of red-orange dots along the posterior border of the tergites and coxal plates. Finally, late pre-ecdysial specimens (stage D2) had a yellowish-orange colour and even better developed red-orange lateral dots. Because the cuticle is relatively thin throughout the entire moult cycle the presence or absence of food in the digestive tract was easy to observe.

Other classification systems exist whereby stage C may be further divided into 4 separate stages, and stage D subdivided into as many as 7 or more individual stages (Drach, 1939**;** Drach and Tchergonovtzeff, 1967**;** Graf, 1986). Essentially, the pre-ecdysial stage D starts

with the secretion of enzyme-containing ecdysial droplets (stage D0) which begin to gradually dissolve away and soften the inner part of the old cuticle. This process starts to free the epidermis from the old overlying cuticle, a process called apolysis, producing an ecdysial cleft (stage D1). Apolysis on the 3rd dactyl of amphipods has been described to occur in stage D (Cornet et al., 2012); as well as in stage C2, with further primitive matrix retraction in the dactylopodite throughout periods C3 and C4 (Graf, 1986). The progressive apolysis in the 3rd dactyl protopodite throughout stage D has been used to subdivide this moulting stage into 7 (Graf, 1986) or 5 (Cornet et al., 2012) separate stages. At the same time the epidermis starts to secrete a new cuticle consisting of an epicuticle and an exocuticle that grows in thickness throughout stages D2 to D4. Meanwhile the old cuticle thins and eventually is shed in the process of ecdysis. The post–ecdysial period is made up of stages A, B and C. Essentially the post-ecdysial period consolidates the new cuticle by secretion of the endocuticle and hardening and thickening of the exocuticle by a combination of mineralisation and sclerotization.

We have previously used X-ray micro-computed (micro-CT) tomography techniques to study various aspects of insect anatomy and physiology (Bell et al., 2012; Greco et al., 2012; Greco et al., 2014; Thielens et al., 2018), including the effect of cadmium on the Malpighian tubules of the seven spotted ladybird (Bell et al., 2012). The current study explored the suitability of this technique to determine the moult stage in a crustacean. Micro-CT identifies changes in the density of radiologically opaque materials such as the degree of calcification of exoskeleton and internal structures. Due to the demands of exoskeleton mineralisation, the calcium requirement will vary depending on the moult cycle stage in crustaceans (see for instance Greenaway, 1985, Wheatley, 1999), and thus has the potential to be a useful tool for moult stage classification. In *Gammarus pulex* there is evidence to suggest that the organism loses about 42% of body calcium into solution over a 2-3-day period preceding the moult and a further 54% is lost with the exuviae, leaving only about 4% in the newly moulted animal (Wright, 1980). The evidence from the measurement of calcium levels in different

tissues including the chitinous exoskeleton and haemolymph at various moult stages and salinities in *Litopenaeus vannamei* (Chun-Huei and Sha-Yen, 2012) would suggest a progressive increase in cuticle calcium concentrations from stages A to mid stage D2 and then a small fall at stage D4 just before ecdysis. During the moult, *G. pulex* specimens shed not only their external exoskeleton, but also the ectodermal lining of their fore gut and hind gut (McLaughin, 1983). Decapods and amphipods have a gastric mill lining their stomachs to aid food mastication and digestion (Icely and Nott, 1992; Schmitz, 1992). The gastric mill consists of a series of gastric ossicles made up of thickened cuticle in the stomach lining which then may or may not be mineralised. Prior to ecdysis it is necessary for calcified gastric ossicles to be shed and dissolved in the animal's gut. Thus, a micro-CT scan of a newly moulted stage A *G. pulex* would be likely to have little or no evidence of calcification of either its exoskeleton or gastric mill. Teleologically the gastric mill, like the exoskeleton, would need to mineralise quickly in stage B and early stage C. During pre-ecdysis, as apolysis took place progressively, at some stage late in stage D, radiological changes should also become apparent in the gastric mill as it became increasingly demineralised prior to moulting.

We hypothesise that because micro-CT identifies differences in radiologically opaque material, such as calcified structures, it will be a useful tool to identify the stage of the moult cycle in *G. pulex*. Thus, the aim was to compare moult stage derivation using micro-CT radiological criteria to the existing established techniques, e.g. 3rd dactyl histology and whole body and eye appearance (Cornet et al., 2012**;** Trevisan et al., 2014) to ascertain the validity of our novel micro-CT scanning method.

2. Materials and methods

2.1. *Gammarus pulex* husbandry and processing

Adult *Gammarus pulex* specimens were collected from the river Cray, Orpington, Kent (51°23'08.8"N 0°06'32.0"E). *G. pulex* were kept at 14ºC with a natural light cycle and fed

leaves collected from the river Cray, and gradually acclimatised over 1 week by replacing ½ of the river water every other day with clean artificial freshwater (AFW) based on the OECD 203 acute toxicity test water with a final salt concentration of 2 mM $CaCl_2$; 0.5 mM $MgSO_4$; 0.8 mM $NaHCO_3$, 77.1 µM KCl, with a measured pH 7.6. Animals were kept in this water for at least 1 week prior to processing for micro-CT scanning. A total of 80 adult *G. pulex* specimens were collected and studied between June 2018 and February 2019. They were fixed via immersion in 4% Paraformaldihyde (PFA) in phosphate buffered saline (PBS). The first 52 specimens, henceforth referred to as the stored/preserved group, were then stored in the preserving fluid for at least 28 days before analysis. The other 28 *G. pulex* specimens studied were assessed immediately after immersion in 4% PFA and are referred to as the fresh sample group (Table 1).

2.2 X-ray micro-computed tomography (micro-CT) scanning

The 80 specimens were carefully blotted to remove excess 4% PFA and then placed in cut-away plastic micro pipettes (VWR European Cat No 129-0296 150X0.05mm) containing dental wax for immobilisation. To prevent excessive dehydration during the scans the specimens had an air-tight small plug of blu tack (Bostik Ltd, Common Rd, Stafford, UK) inserted in the top of the cut-away pipette.

All specimens were scanned using micro-CT scanner (Skyscan 1072 scanner, Bruker Micro-CT, Belgium) using setting described in Tarplee and Corps (2008). The first 15 were scanned at a setting of 61 µA and 73 kV while the remaining 65 specimens were scanned at a setting of 40 µA and 98 kV (see Table 1 for details). No aluminium filter was used at either setting. A flat field correction was made daily before commencing scanning. Depending on the size of the individual specimen, the magnification factor varied from 22X to 40X, the latter magnification being equivalent to an X, Y interpixellar distances of 7.32 µm. All scans where performed isotropically to ensure the inter-slice thickness was the same as the X, Y

151 interpixellar distance. The scan time of the micro-CT scans was 1 hour and 15 min and data
152 stored as 16bit data.
153
154 **2.3 Visualisation Software**
155 The 80 micro-CT scans were converted to axial slices using Skyscan's NReCon software
156 (Bruker Micro-CT, Belgium) and the axial, coronal and sagittal slices were viewed in
157 Tomomask software (www.Tomomask.com; Greco et al., 2014) then straightened to
158 standardise comparisons between individual specimens. The resulting micro-CT scans were
159 viewed with the 3-D viewing software 'disect' (Greco et al., 2014) and the sex of each
160 individual *G.pulex* determined. In the case of the female specimens, the presence or
161 absence of eggs in their brood pouches was also established. For each of the 80 specimens
162 maximum intensity projection (MIP) were obtained to assess the degree of opacification (a
163 measure of calcification) of the internally situated gastric ossicles making up the gastric mill
164 and the exoskeleton and used to assign a moult stage, A, B, C, D or late D. The micro-CT
165 scans of individual organisms were assessed by two researchers independently and
166 assigned a moult-stage classification.
167 .
168 **2.4. Compound microscopic examination of the 3rd dactyl in the stored/preserved**
169 **group and fresh sample group**
170 In 22 of the 52 specimens in the stored/preserved group and all of the 28 specimens of the
171 fresh sample group the 3rd dactyl was removed and examined under a light microscope at
172 200X magnification and its moult stage classified as stage A,B,C or D using the published
173 criteria, Cornet et al., (2012). To confirm accurate moult stage classification using the 3rd
174 dactyl morphology the 3rd dactyl of each specimen was assessed by two researchers
175 independently and assigned a moult-stage classification.
176 .
177

178 **2.5. Dissecting microscopic examination of the external appearance and eye in the**
179 **stored/preserved group and fresh sample group**
180 In 33 of the 52 samples in the stored/preserved group and 27 out of the 28 fresh sample
181 group the external appearance and eye was examined and photographed using a DM350C
182 camera (GT Vision Ltd, Suffolk) under a dissecting microscope and staged according to the
183 criteria of Trevisan et al., (2014). In one of the 28 specimens of the fresh sample group
184 microscopic examination was performed after 24 h of fixation. Photographs of both the left
185 and right lateral views were taken at either 5 or 10X magnification before 15X magnification
186 photographs were obtained of the eye. Individual organisms where assessed by two
187 researchers independently and assigned a moult-stage classification.
188
189 **3. Results**
190 **3.1. Radiological assessment overview**
191 In all 80 scanned specimens visualisation of the external features, as well as internal
192 features such as the gastric mill, radio-opaque material in the gastrointestinal tract were
193 obtained and used to assign to the various stages of moult A, B, C, D and late D (Figs 1 - 8).
194 Visualisation in the 65 specimens scanned at a setting of 40 μA and 98 kV was clearer than
195 in the first 15 scanned at a setting of 61 μA and 73 kV.
196
197 **3.2. *Gammarus pulex* - anatomical studies**
198 Of the 80 scanned specimens, 53 were males and 27 females. The mean (±SD) length of
199 the male specimens from rostrum to telsom was 12.02 (±1.83) mm which was significantly
200 bigger than the females (10.03 (± 1.65) mm, $p < 0.025$). In all but two of the 27 females, eggs
201 were present in their brood pouches (see Figs 7c and 8b).
202
203 The appearance and criteria for classification into moult stages A, B, C, D and late D are
204 provided in Figs 1 to 8 and the accompanying figure legends. At stage A the external
205 exoskeleton and internal gastric mill contained relatively little radio-dense calcium (Fig 1).

Subsequently, as calcium was progressively laid down the degree of radiological opacification in both the exoskeleton and gastric mill increased progressively through stage B (Fig 2) and stage C (Figs 3, 4, 5 and 6). In stage B and C this opacification was most obvious where two sections of the exoskeleton overlapped giving a double shadow such as between adjacent thoracic and abdominal periomeres (Fig 3) or between these structures and coxal plates (Fig 4 and 5). In contrast, in stage D the radiological opacification became more generalised (Fig 6 and 7). Furthermore, in late stage D this more generalised opacification became noticeably defused and less distinct (Fig 8). The calcification in the gastric ossicles making up the gastric mill was absent from both specimens deemed radiologically to be stage A and in the three specimens classified as stage B. All 34 specimens deemed to be radiologically stage C had a normally calcified gastric mill as did all 17 specimens classified radiologically to be early stage D. In contrast in the 24 late stage D specimens 19/24 (79.2%) had indistinct gastric mills and 1/24 (4.2%) had virtually no calcification at all in this structure (see Figure 8c). Using these radiological criteria, the numbers of specimens in the 5 radiological moult stages A, B, C, D and late D were 2 (2.5%), 3 (3.7%), 34 (42.5%), 17 (21.3%) and 24 (30%) respectively.

3.3. Comparison of radiological moult criteria with histological examination of 3rd dactyl

In 50 of the 80 specimens (22 and 28 specimens in the stored/preserved and fresh sample groups, respectively) that were micro-CT scanned a histological examination of the 3rd dactyl was also performed. In 48/50 the claw specimens were of good enough quality to be classified using a combination of the criteria of Cornet et al., (2012) into one of 4 moult stages A, B, C, or a combined early D plus late D stage. Our radiological moult criteria (see Fig 1- 8 and Table 1) agreed with the 3rd dactyl criteria in 48/48 (100%) of the specimens tested.

3.4. Comparison of radiological moult criteria with dissecting microscope whole body and eye appearance

In all 30 specimens in the stored/preserved group the general external appearance as well as eye appearance criteria used by Trevisan et al., (2014) as a moult stage classification tool proved unsatisfactory due to loss of pigmentation following fixation over the 28 days. By way of contrast, in 27 out of 28 in the fresh sample group (<24 h fixation) moult classification using this method was possible. In the one fresh sample group the observation was delayed to >24 h. Interestingly, this relatively short period of extension in the preservative resulted in the removal of body colour and rendered the eye a dark brown rather than black colour meaning it could not be classified. In the 27 samples in the fresh sample group examined immediately after immersion in the 4% PFA solution we were unable to adequately use eye appearance to aid moult stage classification, with only 37% matching the radiological classification (see Table 1). This was because the eyes that were black with white spots were found to be in both stage C and D specimens, which contrasts to Trevisan et al., (2014) classification where these organisms would be in stage B. In comparison the methods of whole-body appearance and micro-CT to classify moult stage was in good agreement, 25/27 (92.5%, see Table 1). In the two specimens where there was disagreement, the method of Trevisan et al., 2014 suggested either moult stage A or B while the radiological method suggested stage C. In both cases the 3rd dactyl examination agreed with the radiological classification rather than the dissecting microscopic appearance (Table 1).

4. Discussion

The study shows for the first time that X-ray micro-CT techniques can be used to determine the moult cycle stage of the freshwater amphipod *Gammarus pulex*. The moult cycle of *G. pulex* is described as lasting from about 15 days (Trevisan et al., 2014) to as many as 30 days (Cornet et al., 2012). These differences in reported moult cycle duration may reflect the fact that the *G. pulex* specimens examined by Trevisan et al., (2014) had a body length of 5 to 8 mm (measured from rostrum to the base of the telson) whereas those studied by Cornet

et al., (2012) were appreciably larger (ranging from 8.45 to 11.90mm in body length), and those in our study were of similar size to those of Cornet et al., (2012). However, the percentage of organisms in stages A, B, C, or stage D reported by Trevisan et al., (2014); 6%, 12%, 40% and 42%, respectively, was comparable to what we found in our 80 specimens of 2.5%, 3.7%, 42.5% and 51.3%.

The radiological technique works equally well in both freshly killed specimens and in those stored in 4% PFA for 28 days. In the process of validating this new method we have also shown that although the method of Trevisan et al., (2014) works well when used to examine live or very recently harvested specimens, in specimens that have been stored for any significant period of time in 4% PFA, the method is unreliable because the preservative decolourises the specimen and changes the colour of the eyes from a predominantly black colour to a dark brown. Even in fresh *G. pulex* samples the eye changes described by Trevisan et al., (2014) can be difficult to interpret if compared to other assessment criteria. This is because small white dots within a predominantly black eye can be seen in stages B and infrequently in stage C (Trevisan et al., 2014), but also in samples that were unequivocally early stage D (Table 1).

The examination of the distal 3rd dactyl as described by several authors (Graf, 1986; Cornet et al., 2012) to determine moult stage worked well when compared to the radiological criteria (100% agreement, Table 1), but from the descriptions it was difficult to distinguish those organisms in later stage of stage C, as opposed to early stage D. Graf, (1986) suggests claw apolysis starts in stage C2 with further dactylopodite apolysis in stage C3 and C4, whilst Cornet et al., (2012) suggests no apolysis occurs until stage D. We found our radiological results better fitted with the 3rd dactyl moult description of Graf, (1986).

G. pulex specimens in stage A had little evidence of radiological opaque calcium in their integumen or gastric mill, however calcium deposition increases in stage B, C and possible

early stage D, as predicted from previous studies (Figs 1-8; Wright, 1980; Greenaway, 1985, Wheatley, 1999). It was also possible to observe that at the end of stage D the amount of calcification in the gastric mill decreased and finally disappears just prior to moulting (Fig 8c). Chisaka and Kozawa., (2003) suggests that in the crayfish *Procambarus clarkii*, the gastric mill calcification consists of the harder hydroxyapatite and not the crystalline form of calcium carbonate (calcite) that is found in the rest of its exoskeleton. The gastric mill is formed from the endocuticle of the stomach and thus the harder crystalline structure of hydroxyapatite may prevent its dissolution by luminal gastric acid (Chisaka and Kozawa, 2003).

Visualisation of the radiological images of the integumental calcification suggests an increase in both early and late stage D when compared with stage C (see Figs 5-8). This was unexpected because apolysis would reduce the thickness and calcium content of the old cuticle during this period. However, a similar result was observed by Chun-Huei and Sha-Yen **(**2012) for the estuarine shrimp, *Litopenaeus vannamei*. Some studies have suggested that approximately 40% of a crustacean's total body calcium is lost when it moults (Wright, 1980) and certainly the current study would support a considerable amount of calcium being lost at the time of ecdyis. Graf and Meyran, (1983, 1985) have described the immediate pre-moult storage of calcium in metal rich granules (MRG) in midgut posterior caeca of a terrestrial crustacean, *Orchestia cavimana*. In *G, pulex*, MRG were observed in the posterior caecae, as well as the posterior parts of the four ventral caeca (Fig. 7 c and d).

5. Conclusion

G. pulex are ecologically important, recycling nutrients through leaf shredding and being a prey item for other organisms. Consequently, they are vital for the functioning of streams and rivers. It has been shown that an increasing number of pollutants may affect moulting as well as reproduction in these amphipods (Gismondi and Thome 2014). Micro-CT scanning enables the moult cycle to be monitored, as well as at the same time being able to visualise integument calcification, internal structures and organs; including egg and embryo

development. Thus, this methodology offers a tool for both ecotoxicologists and invertebrate physiologists to study a variety of life-history traits and physiological responses in one process.

Conflict of Interest: All authors declare no conflict of interest.

References

Bell, G.D., Woolnough, L., Mortimore, D., Corps, N., Hudson, D., Greco, M.K., 2012. A preliminary report on the use of bench top micro-computerised tomography to study the malpighian tubules of the overwintering seven spotted ladybird *Coccinella septempunctata* L. (Coleoptera: Coccinellidae) Psyche, 348, 1-6.

Chisaka, H., Kozawa, Y. 2003. Fine structure and mineralization of the gastric mill in the crayfish *Procambarus clarkii* during the intermoult stage. J. Crust. Biol. 23, 371.-379

Chun-Huei, L., Sha-Yen, C. 2012. Variation of calcium levels in the tissues and hemolymph of *Litopenaeus vannamei* at various moulting stages and salinities
J. Crust. Biol., 32, 101-108.

Cornet, S, Luquet, G., Bollache, L., 2012. Influence of female moulting status on pairing decisions and size-assortative mating in amphipods. J. Zool. 286, 312-319.

Drach, P., 1939. Mue et cycle d'intermue chez les crustaces Decapodes.Annales de l'Institut Oceanographiquie 19, 103 -392.

Drach, P., Tchergonovtzeff, C. 1967. Sur la methode de determination des stades d'intermue et son application generale aux crustaces. Vie et Milieu. Serie A. Biologie

Gismondi, E., Thome, J.2014. Effects of two PBDE congeners on the moulting enzymes of the freshwater amphipod *Gammarus pulex*. Environ. Pollut. 191, 119-125.

Graf, F., 1986. Fine determination of the moult cycle stages in *Orchestia cavimana* Heller (Crustacea: Amphipoda). J. Crust. Biol. 6, 666-678.

343 Graf, F., Meyran, J.C. 1983. Premolt calcium secretion in midgut posterior ceca in a
344 terrestrial crustacean, *Orchestia cavimana* – ultrastructural changes in the postexuvial
345 epithelium. J. Morphol. 177, 1-23.
346 Graf, F., Meyran, J.C. 1985. Calcium reabsorption in the posterior ceca of the midgut in a
347 terrestrial crustacean, *Orchestia cavimana*-ultrastructural changes in the postexuvial
348 epithelium. Cell Tissue Res., 242, 83-95.
349 Greco, M.K., Tong, J., Soleimani, M., Bell, G.D., Schafer, M.O., 2012. Imaging live bee
350 brains using minimally-invasive diagnostic radioentomology. J. Insect Sci. 12, 1-7.
351 Greco, M.K., Woolnough, L., Laycock, S., Corps, N., Mortimore, D., Hudson, D. 2014. 3-D
352 visualisation printing and volume determination of the tracheal respiratory system in the adult
353 desert locust*, Schistocerca gregaria*. Entomol. Exp. Appl. 152, 42-51.
354 Greenaway, P. 1985. Calcium balance and moulting in the Crustacea. Biol. Rev. 60, 425-
355 454.
356 Icely, J.D., Nott, J.A. 1992. Digestion and absorption: Digestive System and associated
357 organs. In Harrison, F.W., Humes, A.G. (Eds), Microscopic Anatomy of Invertebrates:
358 Decapod Crustaceans, Volume 10. Wiley-Liss, New York, pp. 147-201.
359 McLaughin, P.A. 1983. Internal anatomy. In Mantel, L.H. (Ed.) The Biology of Crustacea.
360 Vol. 5. Academic Press, New York, pp 1-52.
361 Schmitz, E.H., 1992. Amphipoda. In Harrison, F.W., Humes, A.G. (Eds.) Microscopic
362 Anatomy of Invertebrates: Crustacea Volume 9. Wiley-Liss, New York, pp.443-528.
363 Tarplee, M., Corps, N 2008. Skyscan 1072 Desktop X-Ray Microtomograph – Sample
364 scanning, reconstruction, analysis and visualisation (2D and 3-D). Protocols. Guidelines,
365 (2008) Notes, selected references and FAQ.
366 Available at: http:/www.geog.qmul.ac.uk/docs/staff/4952.pdf
367 Thielens, A., Bell, G.D., Mortimore, D.G., Greco, M.K., Martens, L., Wout J., 2018. Exposure
368 of insects to Radio-Frequency Electromagnetic Fields from 2 to 120GHz. Sci. Rep. 8, 3924

369 Trevisan, M., Leroy, D., Decloux, N., Thome, J., Compere, P. 2014. Moult-related changes in
370 the integument, midgut, and the digestive gland in the freshwater amphipod *Gammarus*
371 *pulex.* J. Crust. Biol. 34, 539-551.
372 Wheatley, M.G. 1999. An overview of calcium balance in Crustaceans. Physiol. Zool. 69,
373 351-382.
374 Wright, D.A. 1980. Calcium balance in pre-moult and post-moult *Gammarus pulex*
375 (Amphipoda). Freshwater Biol. 10, 571-579.
376
377
378
379

380 **Table 1** Summary of sample preparation, Micro-CT settings, moult stage determination and
381 comparison between assessment methodologies.

			Moult stage assessment methodology				Comparison between moult stage classification via different assessment methodology					
	Amps/ volts (μA/ kV)	Preservation period (Days)	3rd dactyl	Body	Eye	Micro-CT	Micro-CT and 3rd dactyl	Micro-CT and body	Micro-CT and eye	3rd dactyl and body	3rd dactyl and eye	Body and eye
1	61/73	› 28	NA	#	=	B						
2	61/73	› 28	NA	#	=	D						
3	61/73	› 28	late D	#	=	late D	Y					
4	61/73	› 28	late D	#	=	late D	Y					
5	61/73	› 28	NA	#	=	D						
6	61/73	› 28	D	#	=	late D	Y					
7	61/73	› 28	D	#	=	D	Y					
8	61/73	› 28	NA	#	=	D						
9	61/73	› 28	C	#	=	C	Y					
10	61/73	› 28	NA	#	=	D						
11	61/73	› 28	D	#	=	late D	Y					
12	61/73	› 28	NA	#	=	late D						
13	61/73	› 28	NA	#	=	B						
14	61/73	› 28	NA	#	=	late D						
15	61/73	› 28	A or B	#	=	A	Y					
16	40/98	› 28	NA	#	=	late D						
17	40/98	› 28	NA	#	=	late D						
18	40/98	› 28	NA	#	=	late D						
19	40/98	› 28	NA	#	=	late D						
20	40/98	› 28	A or B	#	=	A	Y					
21	40/98	› 28	D	#	=	late D	Y					
22	40/98	› 28	NA	#	=	late D						
23	40/98	› 28	D	#	=	late D	Y					
24	40/98	› 28	D	#	=	late D	Y					
25	40/98	› 28	NA	#	=	late D						
26	40/98	› 28	NA	#	=	D						
27	40/98	› 28	NA	#	=	late D						
28	40/98	› 28	D	#	=	late D	Y					
29	40/98	› 28	D	NA	NA	late D	Y					
30	40/98	› 28	NA	NA	NA	late D						
31	40/98	› 28	NA	NA	NA	late D						
32	40/98	› 28	D	NA	NA	late D	Y					
33	40/98	› 28	D	NA	NA	late D	Y					
34	40/98	› 28	NA	NA	NA	C						
35	40/98	› 28	NA	NA	NA	C						
36	40/98	› 28	NA	NA	NA	D						
37	40/98	› 28	NA	NA	NA	C						
38	40/98	› 28	NA	NA	NA	D						
39	40/98	› 28	NA	NA	NA	late D						
40	40/98	› 28	NA	NA	NA	C						
41	40/98	› 28	NA	NA	NA	C						
42	40/98	› 28	NA	NA	NA	C						
43	40/98	› 28	NA	NA	NA	late D						
44	40/98	› 28	NA	NA	NA	D						
45	40/98	› 28	NA	NA	NA	D						
46	40/98	› 28	C	NA	NA	C	Y					
47	40/98	› 28	C	NA	NA	C	Y					
48	40/98	› 28	C	NA	NA	C	Y					
49	40/98	› 28	D	NA	NA	D	Y					
50	40/98	› 28	D	NA	NA	D	Y					
51	40/98	› 28	D	NA	NA	D	Y					
52	40/98	› 28	C	NA	NA	D	Y					

53	40/98	‹1	C	A or B	A or B	C	Y	N	N	N	N	Y
54	40/98	‹1	C	C	B	C	Y	Y	N	Y	N	N
55	40/98	‹1	C	C	B	C	Y	Y	N	Y	N	N
56	40/98	‹1	NA	A or B	B	C		N	N	NA	NA	Y
57	40/98	‹1	C2	C	B	C	Y	Y	N	Y	N	N
58	40/98	‹1	NA	C	B	C		Y	N	NA	NA	N
59	40/98	‹1	C2	C	B	C	Y	Y	N	Y	N	N
60	40/98	‹1	C2	C	B	C	Y	Y	N	Y	N	N
61	40/98	‹1	C2	C	B	C	Y	Y	N	Y	N	N
62	40/98	‹1	C2	C	B	C	Y	Y	N	Y	N	N
63	40/98	‹1	C2	C	B	C	Y	Y	N	Y	N	N
64	40/98	‹1	C2	C	B	C	Y	Y	N	Y	N	N
65	40/98	‹1	C2	C	B	C	Y	Y	N	Y	N	N
66	40/98	‹1	C	C	C or D	C	Y	Y	Y	Y	Y	Y
67	40/98	‹1	C2	C	B	C	Y	Y	N	Y	N	N
68	40/98	1	A or B	A or B	NA	B	Y	Y		Y		
69	40/98	‹1	D	D	B	D	Y	Y	N	Y	N	N
70	40/98	‹1	D	D	D	D	Y	Y	Y	Y	Y	Y
71	40/98	‹1	D	D	B	D	Y	Y	N	Y	N	N
72	40/98	‹1	late C	D	B	C	Y	N	N	N	N	N
73	40/98	‹1	C	C	C	C	Y	Y	Y	Y	Y	Y
74	40/98	‹1	C	C	C	C	Y	Y	Y	Y	Y	Y
75	40/98	‹1	C	C	B or C	C	Y	Y	Y	Y	Y	Y
76	40/98	‹1	C	C	B or C	C	Y	Y	Y	Y	Y	Y
77	40/98	‹1	C	C	B or C	C	Y	Y	Y	Y	Y	Y
78	40/98	‹1	C	C	B or C	C	Y	Y	Y	Y	Y	Y
79	40/98	‹1	C	C	B or C	C	Y	Y	Y	Y	Y	Y
80	40/98	‹1	C	C	C	C	y	Y	Y	Y	Y	Y
					% agreement between different staging methods		48/48 = 100%	25/27 = 92.5%	10/27 = 37%	24/26 = 92.3%	10/25 = 40%	12/27 = 47%

Y = correct comparisons; N = incorrect comparisons; NA, not accessed; #, impossible due to loss of pigment; =, unable to assess as eyes brown not black with white dots

Legend to figures

Figure 1 (a) A X-ray micro-CT scan showing a 3-D surface volume view of a female *G. pulex*. There is very little evidence of calcification in its exoskeleton suggesting stage A or B. (b) A maximum intensity projection (MIP) 3-D volume view of the same *G.pulex* shown in (a). The gastric mill is not seen in the area indicated by the white arrow suggesting this specimen is stage A. The histology of the iodine stained 3rd dactyl also suggested stage A or B (Table 1).

Figure 2 (a) Right lateral 3-D volume views showing overlapping areas between dorsal plates of thoracic periomeres and abdominal pleomeres relatively indistinct (short white arrow) and line of costal plates hardly visible (long white arrow) due to lack of calcification of the exoskeleton suggests stage B. (b) Dorsal maximum intensity projection view of the same specimen shown in (a). The gastric mill (black arrow) is relatively faintly calcified. The partially calcified gastric mill and histology of the specimen's 3rd dactyl (Table 1) would seem to confirm this is an animal in Stage B.

Figure 3 (a) 3-D volume view showing calcification in overlapping dorsal pereiomeres and pleomeres (white arrows) still relatively faint but greater than in Figs 1a and 2a suggesting early stage C. (b) Dorsal maximum intensity projection view of the same specimen as seen in (a). The gastric mill is now densely calcified (arrow 1) while maximum opacification is seen where the dorsal pereiomeres and pleomeres overlap (arrow 2). The overlapping sternal plates of abdominal pleomeres are faintly seen (arrow 3) again suggesting early stage C.

Figure 4 (a). 3-D volume view of a specimen judged to be early stage C. Not only are the white areas between overlapping dorsal plates of the thoracic periomeres and abdominal pleomeres (black arrow 1) now seen clearly, also the overlapping areas between the coxal plates and periomeres are becoming more distinct than in Fig. 3a (black arrow 2). (b) Dorsal

maximum intensity projection view of the same specimen as shown in (a). The gastric mill is fully calcified (arrow 1) and the overlapping sternal plates in the thoracic (arrow 2) and abdominal areas (arrow 3) are more distinct than in Fig 3b.

Figure 5. A later stage C specimen with calcification in the centre of the coxal plates (black arrow 3) as well as calcification in the overlapping dorsal and pereiomeres and pleomeres (black arrow 2) and 'coxal line' (black arrow 1).

Figure 6 (a) Later Stage C slightly more advanced than specimen shown in Fig 5 with calcification not only in coxal plates (white arrow 1) but also early calcification in the head capsule (white arrow 2). (b) Left lateral dorsal maximum intensity projection view of the same specimen as seen in (a) showing faint mottled calcification in the head capsule (white arrow 1) and similarly faint calcification in the middle of the abdominal pleomeres (white arrow 2). Note also calcification in the joints between the sections of the pereiopods and uropods (white arrow 3), as well as a densely calcified gastric mill (white arrow 4)

Figure 7 (a) Stage D with more extensive calcification of the exoskeleton than previous figures in stage C. (b) Doral maximum intensity projection view of the same specimen as shown in (a) showing a dispersed 'fuzzy' appearance to the calcified exoskeleton and the gastric mill is becoming indistinct. (c) 2-D midline sagittal and transverse views respectively showing metal rich granules (MRG) (white arrow 1) and this specimen also has multiple eggs in her brood patch (white arrow 2). (d) MRG (white arrows) in the dorsally placed pair of posterior caecae which arise at the junction of the mid gut and hind gut and then pass anteriorly along the dorsal surface of the mid gut. Annular radio-opaque material is also seen at 9 o'clock, 3 o'clock and at both 5 and 7 o'clock. This represents MRG in the walls of the 4 ventral caecae.

Figure 8 (a) Female in very late in moult stage D with extensive dispersed 'fuzzy' calcification. (b) Lateral 2-D sagittal view of the same female specimen as (a) showing eggs with calcified rims in her brood pouch (longer white arrows) and extensive dorsal separation between the old and new cuticle (shorter white arrow). (c) Enlarged maximum intensity projection view of the same female specimen showing that the gastric mill has virtually disappeared apart from a very thin rim in two separate halves (white arrow).

Figure 1

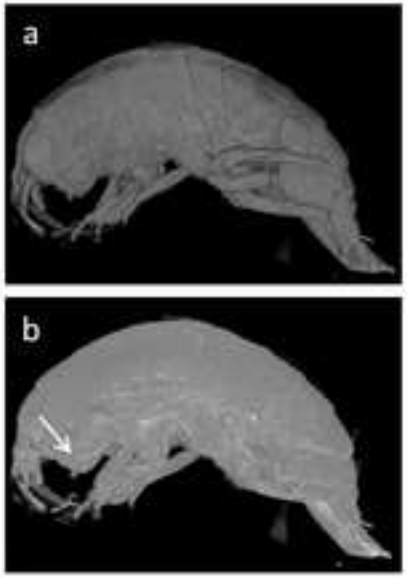

Figure 2

Click here to access/download;Figure;Figure 2.tif

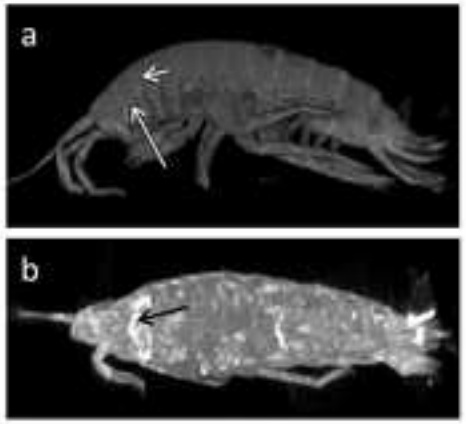

Figure 3

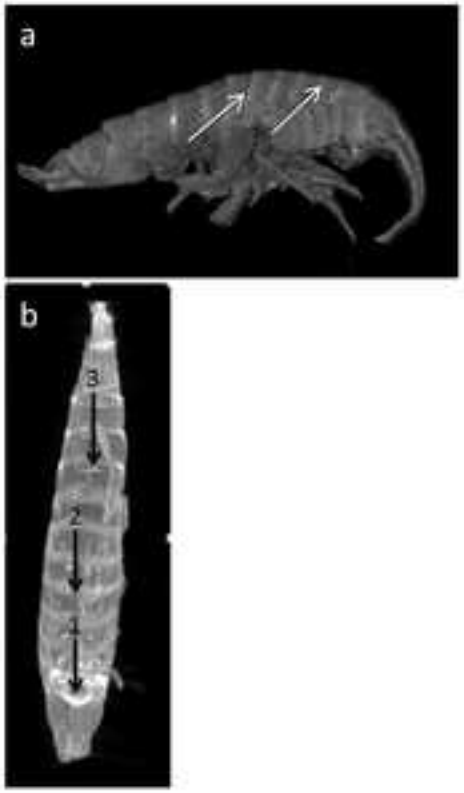

Figure 4

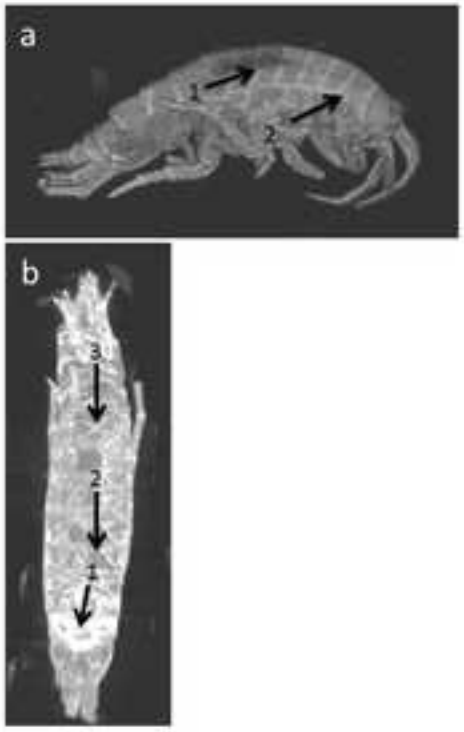

Figure 5

Click here to access/download;Figure;Figure 5.tif

Figure 6

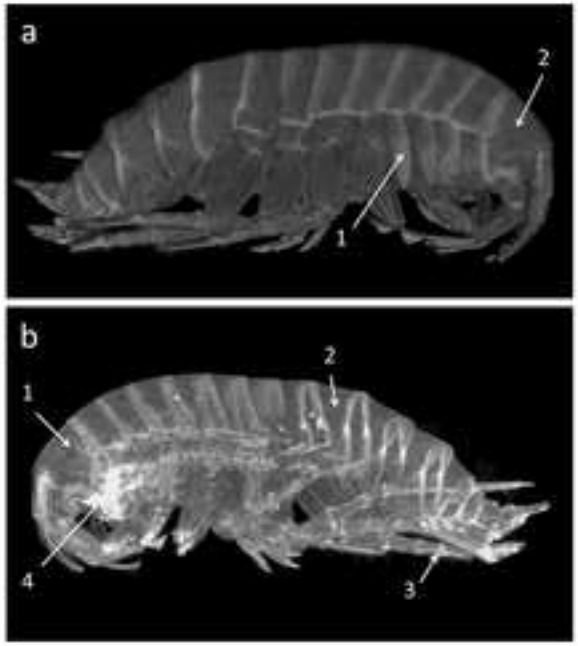

Figure 7

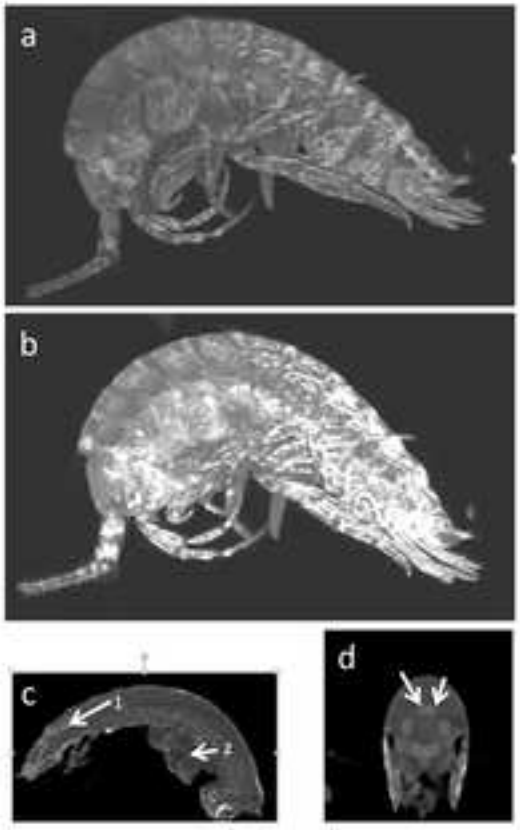

Figure 8

Click here to access/download;Figure;Figure 8.tif